Euro. Jnl of Applied Mathematics (2011), *vol.* 22, *pp.* 217–243.
doi:10.1017/S0956792511000039

On continuous branches of very singular similarity solutions of a stable thin film equation. I – The Cauchy problem

J. D. EVANS and V. A. GALAKTIONOV

Department of Mathematical Sciences, University of Bath, Bath, BA2 7AY, UK
email: masjde@maths.bath.ac.uk, vag@maths.bath.ac.uk

(*Received 5 March 2010; revised 16 December 2010; accepted 6 January 2011; first published online 21 February 2011*)

We consider the fourth-order thin film equation,

$$u_t = -\nabla \cdot (|u|^n \nabla \Delta u) + \Delta(|u|^{p-1}u), \text{ where } n > 0,\ p > 1,$$

with a *stable* second-order diffusion term. For the first critical exponent,

$$p = p_0 = n + 1 + \frac{2}{N} \quad \text{for } n \in \left(0, \frac{3}{2}\right),$$

where $N \geqslant 1$ is the space dimension, the Cauchy problem is shown to admit countable continuous branches of source-type self-similar *very singular* solutions of the form

$$u(x,t) = t^{-\frac{N}{4+nN}} f(y), \quad y = x/t^{\frac{1}{4+nN}}.$$

These solutions are inherently oscillatory in nature and will be shown in Part II to be the limit of appropriate free-boundary problem solutions. For $p \neq p_0$, the set of very singular solutions is shown to be finite and to be consisting of a countable family of branches (in the parameter p) of similarity profiles that originate at a sequence of critical exponents $\{p_l,\ l \geqslant 0\}$. At $p = p_l$, these branches appear via a non-linear bifurcation mechanism from a countable set of similarity solutions of the *second kind* of the pure thin film equation

$$u_t = -\nabla \cdot (|u|^n \nabla \Delta u) \quad \text{in} \quad \mathbb{R}^N \times \mathbb{R}_+.$$

Such solutions are detected by the 'Hermitian spectral theory', which allows an analytical n-branching approach. As such, a continuous path as $n \to 0^+$ can be constructed from the eigenfunctions of the linear rescaled operator for $n = 0$, i.e. for the bi-harmonic equation $u_t = -\Delta^2 u$. Numerics are used, wherever appropriate, to support the analysis.

Key words: Stable thin film equation; Cauchy problem; Global similarity solutions; Asymptotic behaviour; Branching; Bifurcations; Hermitian spectral theory

1 Introduction: the stable thin film equation and main results

1.1 The model and preliminary discussion

We study the large time behaviour of solutions of high-order, quasi-linear degenerate parabolic equations that are in non-divergent form. More precisely, we construct global in time, self-similar, *very singular solutions* (VSS) of the fourth-order quasi-linear parabolic *thin film equation* (TFE-4) with a *stable* homogeneous second-order diffusion term,

$$u_t = -\nabla \cdot (|u|^n \nabla \Delta u) + \Delta(|u|^{p-1}u), \quad \text{where } n > 0 \text{ and } p > 1. \tag{1.1}$$

We treat here the Cauchy problem (CP) for (1.1), by which we mean those solutions that admit maximal regularity as they vanish at a singularity surface (interface) $\Gamma_0[u]$, which is the lateral boundary of $\operatorname{supp} u \subset \mathbb{R}^N \times \mathbb{R}_+$. The problem is completed with bounded, smooth, integrable, compactly supported initial data in $\mathbb{R}^N$, namely

$$u(x,0) = u_0(x) \quad \text{in } \Gamma_0[u] \cap \{t = 0\}. \tag{1.2}$$

For clarity, we leave the discussion of closely associated Free-Boundary Problems (FBPs) until the Part II companion paper, though it should be mentioned that these two problem classes are inextricably linked.

The present results of Parts I and II complete the analysis of the TFEs performed in [9,10], where countable sets and continuous branches of *blow-up* and *global* similarity solutions were obtained for the *limit unstable TFE* with the *backward diffusion* parabolic term

$$u_t = -\nabla \cdot (|u|^n \nabla \Delta u) - \Delta(|u|^{p-1}u) \quad (n > 0, \ \ p > 1). \tag{1.3}$$

The main mathematical approaches for (1.3) are similar to those applied in [11] to the sixth-order limit unstable TFE-6,

$$u_t = \nabla \cdot (|u|^n \nabla \Delta^2 u) - \Delta(|u|^{p-1}u) \quad (n > 0, \ \ p > 1). \tag{1.4}$$

Surveys and extended lists of related references on the physics and mathematics of such thin film partial differential equations (PDEs) can be found in [9] and [11]. Regarding our analysis, we mention the key pioneering papers for high-order non-linear diffusion theory in the 1990s by Bernis [1], Bernis and Friedman [2] (mainly, FBP theory for TFEs), and Bernis and McLeod [4], where oscillatory similarity solutions of the CP for the fourth-order porous medium-like equations (the PMEs-4) were constructed. Also see Bernis *et al.* [5], Ferreira and Bernis [13]. Further details can also be found in the monograph by Wu *et al.* [28, Ch. 4].

We begin our study in the critical 'conservative' case,

$$p = p_0 = n + 1 + \frac{2}{N}, \tag{1.5}$$

which is easier to analyse technically and reveals specific properties of similarity patterns. Eventually, we extend our approach to $p \neq p_0$ (more precisely, for $p < p_0$). It is worth

https://doi.org/10.1017/S0956792511000039 Published online by Cambridge University Press

noting that (1.1) for $n = 0$ is the *limit stable Cahn–Hilliard equation*,

$$u_t = -\Delta^2 u + \Delta(|u|^{p-1}u), \tag{1.6}$$

which occurs in various applications (see references in [12]).

1.2 Main results and layout of the paper

We construct very singular self-similar (or source-type for $p = p_0$) solutions of (1.1) in certain ranges of the parameters n, p and N. For small enough $n > 0$, we will often refer to analogies with the semi-linear Cahn–Hilliard equation (1.6). Typically, we assume that

$$n \in \left[0, \tfrac{3}{2}\right) \quad \text{and} \quad p > n + 1, \tag{1.7}$$

but in places we also treat $n > \frac{3}{2}$, for which the CP continues to admit sign changing solutions that are infinitely oscillatory at the interfaces.

In Section 2 we formulate the similarity setting of the problem. Our conclusions and further layout of the paper are as follows.

We show that the stable TFE (1.1) admits the following:

(i) In the critical case $p = p_0$, continuous families of global similarity solutions (Section 3).

(ii) As a co-product, we study in Section (4) the countable set of similarity solutions of the pure TFE (these define special bifurcation values $\{p_l\}$ for the full model (1.1)),

$$u_t = -\nabla \cdot (|u|^n \nabla \Delta u) \quad \text{in} \quad \mathbb{R}^N \times \mathbb{R}_+. \tag{1.8}$$

The analysis begins with the linear problem for $n = 0$, i.e. for the *bi-harmonic equation*,

$$u_t = -\Delta^2 u, \tag{1.9}$$

where a form of the *Hermitian spectral theory* is developed in Section 4.1 for linear rescaled operators of the CP.

(iii) For $p < p_0$ (for $p > p_0$ no such VSS exists), the number of similarity solutions (for a given p value) becomes finite, and there exists a countable family of p-branches[1] of similarity profiles that originate at certain non-linear bifurcation points $\{p_l > 1,\ l \geqslant 0\}$ (Section 5).

Finally, we claim that similar principles of self-similar asymptotics apply to the sixth-order stable TFE (see [11] for such models and references),

$$u_t = \nabla \cdot (|u|^n \nabla \Delta^2 u) + \Delta(|u|^{p-1}u) \tag{1.10}$$

for $n \in [0, \frac{5}{4})$. In this case, the first critical exponent is $p_0 = n + 1 + \frac{4}{N}$. The semi-linear case $n = 0$ leads to the sixth-order limit unstable Cahn–Hilliard equation,

[1] See [12, 16, 18, 21] as a source of a detailed construction of such branches in various problems for bi-harmonic and thin film PDEs.

https://doi.org/10.1017/S0956792511000039 Published online by Cambridge University Press

$$u_t = \Delta^3 u + \Delta(|u|^{p-1}u), \tag{1.11}$$

whose similarity solutions can be studied as in [12].

2 Global similarity solutions: general statement and preliminaries

The similarity solutions of (1.1) have the form

$$u_S(x,t) = t^{-\alpha} f(y), \quad y = x/t^{\beta}, \quad \text{with} \quad \alpha = \frac{1}{2p-(n+2)} > 0, \ \beta = \frac{p-(n+1)}{2[2p-(n+2)]} > 0. \tag{2.1}$$

The function f solves a quasi-linear elliptic equation, namely

$$\mathbf{A}_+(f) \equiv -\nabla \cdot [|f|^n \nabla \Delta f - \nabla(|f|^{p-1}f)] + \beta y \cdot \nabla f + \alpha f = 0. \tag{2.2}$$

For $n > 0$, a natural functional setting for the CP includes the condition

$$f(y) \quad \text{is non-trivial in a bounded domain in } \mathbb{R}^N. \tag{2.3}$$

In the CP, $f(y)$ can be extended by $f(y) \equiv 0$ outside the support. It is also noteworthy for the CP that the elliptic equation (2.2) admits non-compactly supported solutions with asymptotics as $y \to \infty$ governed by the leading linear first-order operator,

$$\beta y \cdot \nabla f + \alpha f + \cdots = 0 \quad \Longrightarrow \quad f(y) = C|y|^{-\frac{\alpha}{\beta}}(1 + o(1)), \tag{2.4}$$

where $C = C(\frac{y}{|y|})$ is an arbitrary smooth function on the unit sphere S^{N-1}. Actually, in order to satisfy the desired condition (2.3), one needs to demand that

$$C = 0 \quad \text{in} \quad (2.4). \tag{2.5}$$

In the case $n = 0$, (2.3) is replaced by

$$f(y), \quad \text{which has exponential decay at infinity (see [12])}, \tag{2.6}$$

meaning that f belongs to a special weighted L^2 space. The condition (2.5) is also necessarily implied.

Under (2.3) (or equivalently (2.6)), integrating (2.1) over $\mathbb{R}^N$ yields the following mass time-dependence for $p \neq p_0$:

$$\int u_S(x,t)\,\mathrm{d}x = t^{\frac{N(p-p_0)}{2[2p-(n+1)]}} \int f(y)\,\mathrm{d}y \quad \Longrightarrow \quad \int f = 0 \quad (p \neq p_0). \tag{2.7}$$

For $p = p_0$, any mass of $f(y)$ is formally allowed; cf. [10].

For general solutions of the TFE-4 (1.1), the self-similar scaling

$$u(x,t) = (1+t)^{-\alpha}\theta(y,\tau), \quad y = x/(1+t)^{\beta}, \quad \tau = \ln(1+t), \tag{2.8}$$

yields the evolution equation with the same operator as in (2.2)

$$\theta_\tau = \mathbf{A}_+(\theta) \quad \text{for} \quad \tau > 0. \tag{2.9}$$

https://doi.org/10.1017/S0956792511000039 Published online by Cambridge University Press

Then a typical asymptotic stabilisation problem occurs as $\tau \to +\infty$, which, in particular, requires to know all possible equilibria of $\mathbf{A}_+$, this being the main current problem of concern.

The critical exponent (1.5) follows from conservation of mass; q.v. the same derivation in [9, Section 3]. In addition, a countable sequence of other critical exponents $\{p_l,\, l = 0, 1, 2, \ldots\}$ is expected to exist. This is confirmed in the semi-linear case $n = 0$ (for the limit Cahn–Hilliard equation (1.6)), where [12, Section 5]

$$p_l = 1 + \frac{2}{N+l} \quad \text{for any} \quad l = 0, 1, 2, \ldots . \tag{2.10}$$

See further comments in [9, Section 2].

3 Local oscillatory ordinary differential equation (ODE) bundles and profiles for $p = p_0$

We study the similarity ODE in the radial setting. Let $y \geqslant 0$ denote the single spatial variable. The operator of (2.1) is then ordinary differential

$$\mathbf{A}_+(f) \equiv -\frac{1}{y^{N-1}} \left[y^{N-1} |f|^n \left(\frac{1}{y^{N-1}} (y^{N-1} f')' \right)' - y^{N-1} (|f|^{p-1} f)' \right]' + \beta y f' + \alpha f = 0. \tag{3.1}$$

We first describe the corresponding oscillatory bundle of asymptotic profiles close to interface points, which are attributed to the CP. For both $n = 0$ and $n > 0$, we then describe the 'Hermitian spectral theory' appropriate to the Cauchy setting in $\mathbb{R}^N$.

3.1 Local oscillatory behaviour close to interfaces

The questions on oscillatory behaviour of changing sign have been considered before. Following [10, Section 7.1], we briefly indicate the oscillatory asymptotic bundle of similarity profiles $f(y)$ exhibiting *maximal regularity* at the interface $y = y_0$, so that on being extended by $f = 0$ for $y > y_0$ these will give solutions of the CP. These may be considered as the counterpart of the smooth similarity solutions of the CP for $n = 0$ [12, Section 5], i.e. we have a regular limit as $n \to 0^+$. It is easy to see that for $n \in (0, \frac{3}{2})$ the ODE (3.2) does not admit non-negative solutions of maximal regularity. Hence, the ODE (3.2) implies that sufficiently regular solutions $f(y)$ must be oscillatory near interfaces; cf. proofs in [4]. It is important to prescribe the precise structure of such oscillatory singularities of the ODE and determine the dimension of the asymptotic bundle.

For $n > 0$, we take the thin film ODE (3.1), keeping the main terms for $y \approx y_0^-$ and integrating once, to obtain

$$|f|^n \left(f'' + \frac{(N-1)}{y} f' \right)' - (|f|^{p-1} f)' = \beta y_0 f + (\text{higher order terms}). \tag{3.2}$$

For $N = 1$, choosing next just two leading terms close to the interface yields (in fact, one can see that this approximation holds for any dimension $N \geqslant 1$)

$$|f|^n f''' = \lambda_0 f + \cdots , \tag{3.3}$$

https://doi.org/10.1017/S0956792511000039 Published online by Cambridge University Press

where $\lambda_0 = \beta y_0$. Thus, we need to consider the unperturbed ODE

$$|f|^n f''' = \lambda_0 f \quad (\lambda_0 = \beta y_0 > 0), \tag{3.4}$$

whose orbits will be exponentially small perturbations near interfaces of those for (3.1).

The ODE (3.4) has the following representation for its solutions [10, Section 7]: as $y \to y_0^-$,

$$f(y) = (y_0 - y)^\mu \varphi(\eta), \quad \eta = \ln(y_0 - y), \quad \text{with } \mu = \frac{3}{n}, \tag{3.5}$$

where the *oscillatory component* φ satisfies the autonomous ODE,

$$\varphi''' + 3(\mu - 1)\varphi'' + (3\mu^2 - 6\mu + 2)\varphi' + \mu(\mu - 1)(\mu - 2)\varphi + \lambda_0 |\varphi|^{-n}\varphi = 0. \tag{3.6}$$

One can see that on orbits like (3.5) the neglected term $(|f|^{p-1}f)'$ in (3.2) is much smaller than f for all $p > 1 + \frac{n}{3}$, and hence also for our range of interest $p > 1 + n$.

We are interested in the *periodic solutions* of (3.6) in the form (3.5), these oscillatory profiles changing sign infinitely often as $y \to y_0^-$, i.e. as $\eta \to -\infty$. Indeed, via (3.5), periodic functions $\varphi_*(\eta)$ establish the *simplest oscillatory connections* with the interface points keeping the maximal regularity of the *envelope*:

$$f(y) \sim (y_0 - y)^{\frac{3}{n}} \quad \text{for} \quad y \approx y_0^-,$$

which represents the true scaling-invariant nature of the ODE (3.4). It can be shown that (3.6) is a dissipative Dynamical System having a bounded absorbing set. Moreover, dissipative dynamical systems are known to admit periodic solutions in a more general setting [25, Section 39], provided these are non-autonomous (so the period is fixed).

According to (3.5), the regularity at $y = y_0$ increases as $n \to 0^+$ forming, at $n = 0$, analytic solutions. In [11, Section 6], we present a discussion related to the theory of periodic solutions for higher order ODEs. Unlike the fifth-order case in [11, Section 4], the ODE (3.6) is of third order and can be reduced to a first-order ODE (see [10, Section 7.1]). Therefore the existence of a periodic solution is not principally difficult, while uniqueness (and stability) are more difficult to show. We expect, and this is confirmed by numerics [10], that this limit cycle is 'almost' globally stable (note that all the orbits of (3.6) are uniformly bounded, so a stable attractor should be available, though sometimes zero may have a stable manifold, which was not observed for this case; however, we have no proof) and is unique.

As n increases, this periodic solution $\varphi_*(s)$ is destroyed in a heteroclinic bifurcation at the point [10, Section 7.2]

$$n_{\rm h} = 1.758665\ldots \quad \left(\text{and } n_{\rm h} \in \left(\frac{3}{2}, n_+\right), \text{ where } n_+ = \frac{9}{3 + \sqrt{3}} = 1.9019238\ldots, \text{ [19]}\right), \tag{3.7}$$

with a standard scenario of homoclinic/heteroclinic bifurcation (see [26, Ch. 4]). A rigorous justification of such non-local bifurcations is an open problem.

Thus, for n larger than $\frac{3}{2}$, not all the solutions are oscillatory near the interfaces. For $n \in (\frac{3}{2}, 3)$, there exists a one-parametric bundle of positive solutions with constant

https://doi.org/10.1017/S0956792511000039 Published online by Cambridge University Press

equilibria $\varphi(\eta) \equiv \pm\varphi_0$ given by

$$\varphi_0 = \left[-\frac{\beta y_0}{\mu(\mu-1)(\mu-2)}\right]^{\frac{1}{n}}. \tag{3.8}$$

For matching purposes though, this is not enough and the whole two-dimensional (2D) asymptotic bundle (3.5) of oscillatory solutions has to be taken into account.

For the CP then, this oscillatory behaviour is expected to remain generic for all $n \in (0, n_{\rm h})$ (and similar to the linear case $n = 0$ with interface at $y_0 = \infty$; see [10]). Explicitly, the 2D bundle of asymptotic oscillatory orbits near the interface has the behaviour

$$f(y) = (y_0 - y)^{\frac{3}{n}} \varphi_*(\ln(y_0 - y) + s_0) + \cdots \quad \text{as} \quad y \to y_0^-, \tag{3.9}$$

where $y_0 > 0$ and $s_0 \in \mathbb{R}$ are parameters.

Another important question is the passage to the limit $n \to 0^+$ that shows convergence to solutions of the semi-linear Cahn–Hilliard equation. This is explained in detail in [10, Section 7.6]. Various oscillatory sign change issues for non-linear degenerate higher order PDEs of different types are addressed in [20, Ch. 3–5].

3.2 Continuous branches of similarity profiles for $p = p_0$

Again, without loss of generality, we treat the case $N = 1$, where the ODE is simpler and takes the form

$$|f|^n f''' - \frac{1}{n+4} yf - (|f|^n f^3)' = 0. \tag{3.10}$$

The origin of the existence of continuous branches (parameterised by, e.g. mass) is the fact that the ODE (3.10) is of third order. Thus, the single symmetry condition

$$f'(0) = 0 \quad (f(0) \neq 0) \tag{3.11}$$

is posed at the origin, while the shooting bundle from the singularity point $y = y_0$ is two dimensional according to (3.9). This leaves one free parameter. Solution existence by a shooting approach is standard, so we refer to [10, 12, 21] as a guide to such equations.

The numerical results below were mainly obtained using `Matlab`'s two-point boundary value problem collocation solver `bvp4c` (with default parameter values RelTol $= 10^{-3}$, AbsTol $= 10^{-6}$). The standard regularisation

$$|f|^n \mapsto (\delta^2 + f^2)^{\frac{n}{2}} \tag{3.12}$$

was used with typically δ taken as 10^{-6} (although values as low as 10^{-10} were used to obtain the complicated and refined zero structure of solutions shown in Figure 4).

In Figure 1, we present similarity profiles for $n = N = 1$ and $p = p_0 = n + 3 = 4$, which are parameterised by values at the origin $f(0)$.

For comparison, in Figure 2(a), we present similar profiles for the semi-linear case $n = 0$, i.e. for the limit Cahn–Hilliard equation (1.6), where $p = p_0 = 3$. Figure 2(b) shows a clear difference of the 'tail' behaviour for $n = 1$ (non-linear oscillations (3.9)) and $n = 0$ (a linearised behaviour).

https://doi.org/10.1017/S0956792511000039 Published online by Cambridge University Press

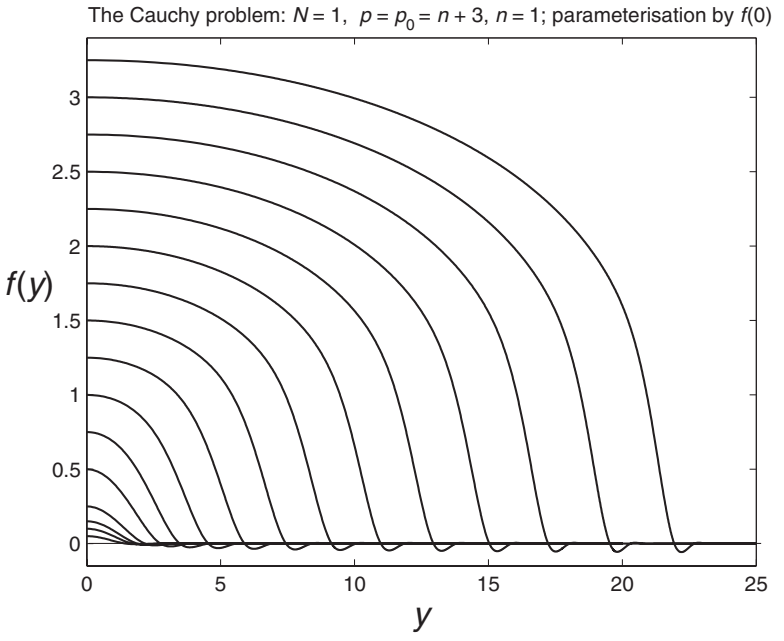

FIGURE 1. Similarity profiles for the CP as solutions of (3.10) and (3.11) for $N = n = 1$, $p = n + 3 = 4$.

In Figure 3, we show how the similarity profiles at $p = p_0 = n + 3$ are deformed with n starting from the semi-linear case $n = 0$. It is seen that the profiles get narrower as n increases and also less oscillatory near their interfaces. In Figure 4, we show their enlarged oscillatory behaviour close to the interfaces. We note that the case $n = 1.75$ is close to the heteroclinic value (3.7) for which the CP profile must still change sign (whilst the corresponding FBP one does not [10]). For subsequent n after the heteroclinic value, the similarity profiles are assumed to be finitely oscillatory, i.e. can have a finite number of sign changes near the interface (or none at all; see further comments in [10, Section 9.4]). This finite oscillation phenomenon is challenging numerically. Our numerics show that for $n = 1.75$, the CP profile still changes sign near the interface (see Figure 4).

In Figure 3, we also include the case of a single negative value $n = -\frac{1}{2}$, which gives a standard source-type profile but, of course, without a finite interface, where $f(y)$ is oscillatory as $y \to +\infty$. The structure of these oscillations at infinity is different from the already known ones for n non-negative, and is not studied here.

4 Countable family of source-type profiles via an n-branching approach

For later convenience, we postpone our study of the original PDE (1.1) and digress to the pure unperturbed TFE. In general, construction of various oscillatory source-type solutions of the CP for *pure* TFE (1.8) is a non-linear problem, which is more difficult than that for the corresponding FBP.

https://doi.org/10.1017/S0956792511000039 Published online by Cambridge University Press

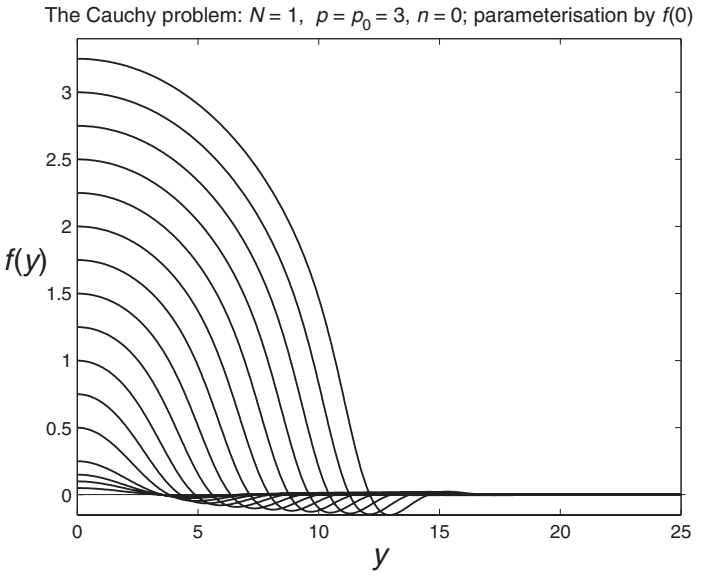

(a) $f(y)$ for $n = 0$

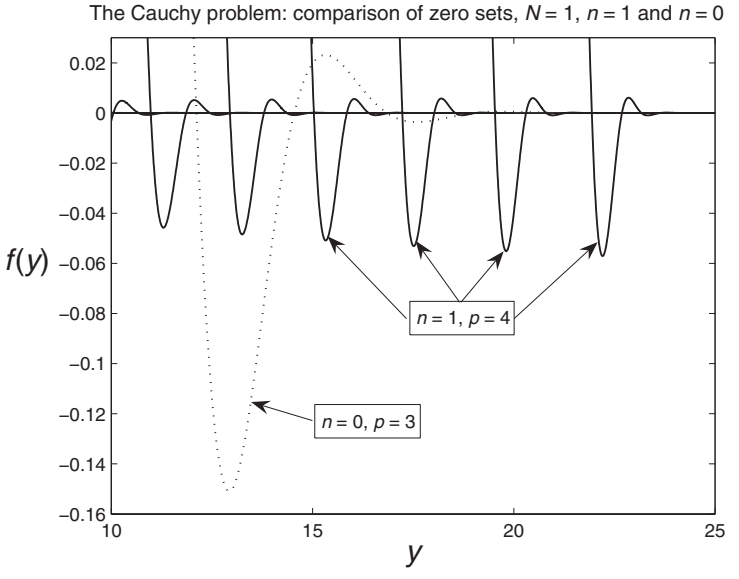

(b) Zero structure enlarged

FIGURE 2. Similarity profiles for the CP satisfying (3.10) and (3.11) for $N = 1$, $n = 0$ $p = 3$; (a) profiles, and (b) zero structure.

4.1 The linear case $n = 0$: basics of Hermitian spectral theory

For $n = 0$, i.e. for the bi-harmonic equation (1.9), the first profile exists, is unique (up to mass scaling) and is just the rescaled kernel $F(y)$ of the fundamental solution of (1.9):

https://doi.org/10.1017/S0956792511000039 Published online by Cambridge University Press

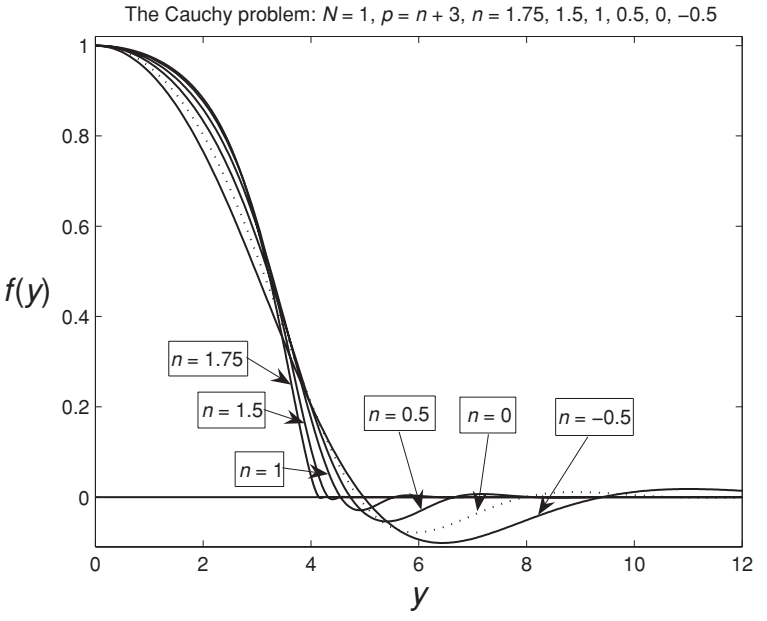

FIGURE 3. Similarity profiles for the CP as solutions of (3.10) and (3.11) for $N = 1$, $p = n + 3 = 4$ and various $n \in [-\frac{1}{2}, 1\frac{3}{4}]$; parameterisation is $f(0) = 1$.

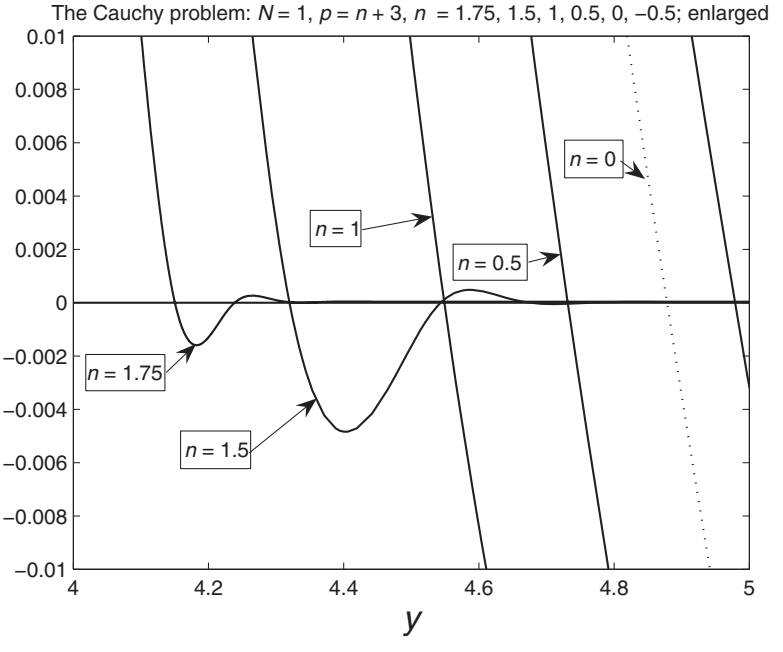

FIGURE 4. Enlarged zero structure of VSS profiles from Figure 3; for $p = 1.75$, $f(y)$ still changes sign.

https://doi.org/10.1017/S0956792511000039 Published online by Cambridge University Press

$$b(x,t) = t^{-\frac{N}{4}} F(y), \quad y = x/t^{\frac{1}{4}}, \quad \text{where}$$
$$\mathbf{B}F \equiv -\Delta^2 F + \tfrac{1}{4}\, y \cdot \nabla F + \frac{N}{4}\, F = 0 \ \text{ in } \mathbb{R}^N, \quad \int F = 1; \tag{4.1}$$

see [9, Section 4]. Moreover, there exists a countable set of eigenfunctions $\{\psi_\gamma,\ l = |\gamma| \geqslant 0\}$ of the corresponding rescaled non-self-adjoint operator $\mathbf{B}$ with the discrete spectrum [8]

$$\sigma(\mathbf{B}) = \left\{ -\frac{l}{4},\ l = 0, 1, 2, \dots \right\}. \tag{4.2}$$

The eigenfunctions are derivatives of the rescaled kernel F,

$$\psi_\gamma(y) = \frac{(-1)^{|\gamma|}}{\sqrt{\gamma!}}\, D^\gamma F(y) \quad \text{for any multi-index } \gamma. \tag{4.3}$$

In addition, the adjoint operator has the same spectrum:

$$\mathbf{B}^* = -\Delta^2 - \frac{1}{4}\, y \cdot \nabla \quad \text{with} \quad \sigma(\mathbf{B}^*) = \sigma(\mathbf{B}) = \left\{ -\frac{l}{4},\ l = 0, 1, 2, \dots \right\}, \tag{4.4}$$

and a complete set of eigenfunctions $\{\psi^*_\gamma(y)\}$, which are *generalised Hermite polynomials*. More details on such Hermitian spectral theory of the operator pair $\{\mathbf{B}, \mathbf{B}^*\}$ is in [8, 15].

4.2 n-branching of similarity solutions

We apply the n-branching approach from the linear case $n = 0$ in order to explain the existence of a countable set of similarity solutions of the TFE (1.8). We will follow classic branching theory in the case of non-analytic non-linearities of finite regularity (see [27, Section 27] and [25, Ch. 8]).

We look for solutions of (1.8) with small $n > 0$ in the standard form

$$u_\gamma(x,t) = t^{-\alpha} f(y), \quad y = x/t^\beta, \quad \text{where} \quad \beta = \frac{1 - \alpha n}{4}, \tag{4.5}$$

where the multi-index γ is used for numbering (in a manner similar to that for the linear eigenfunctions (4.3) and which is explained below). Then $f = f_\gamma(y)$ solves the elliptic equation

$$\mathbf{A}_n(f) \equiv -\nabla \cdot (|f|^n \nabla \Delta f) + \beta y \cdot \nabla f + \alpha f = 0 \quad \text{in} \quad \mathbb{R}^N. \tag{4.6}$$

Note that, in general, for $l = |\gamma| \geqslant 1$, we have to assume that

$$\int f(y)\, \mathrm{d}y = 0 \tag{4.7}$$

so that the solutions (4.5) satisfy the mass conservation condition

$$\int u_\gamma(x,t)\, \mathrm{d}x \equiv 0 \quad (|\gamma| \geqslant 1). \tag{4.8}$$

https://doi.org/10.1017/S0956792511000039 Published online by Cambridge University Press

For $l = 0$, where $\alpha = \beta N$ and $\beta = \frac{1}{4+nN}$, the assumption (4.7) is not necessary, since the PDE (4.6) is fully divergent and admits integration over $\mathbb{R}^N$.

For small $n > 0$ in (4.6), we have

$$\beta = \frac{1}{4} - \frac{\alpha}{4} n, \tag{4.9}$$

and we use the following expansion:

$$|f|^n = 1 + n \ln |f| + o(n). \tag{4.10}$$

Here, (4.10) should be understood in the weak sense, which is necessary for use in the equivalent integral equation (see below).

Substituting expansions (4.9) and (4.10) (still completely formal) into (4.6) yields

$$\mathbf{A}_n(f) \equiv \mathbf{B}f + \big(\alpha - \frac{N}{4}\big) f + n\mathscr{L}(f) + o(n) = 0, \tag{4.11}$$

with the perturbation operator

$$\mathscr{L}(f) = -\nabla \cdot \Big(\ln |f| \nabla \Delta f \Big) - \frac{\alpha}{4} y \cdot \nabla f. \tag{4.12}$$

We next describe the behaviour of solutions for small $n > 0$ and apply the classical Lyapunov–Schmidt method [25, Ch. 8] to (4.11). In this linearised setting, we naturally arrive at the functional framework that is suitable for the linear operator $\mathbf{B}$, i.e. it is $L^2_\rho(\mathbb{R}^N)$, with the domain $H^4_\rho(\mathbb{R}^N)$ etc., and a similar setting for the adjoint operator $\mathbf{B}^*$ (see above and further details in [8]).

Therefore, for $n = 0$, we have to study the branching of a non-linear eigenfunction from the linear one, where f is a certain non-trivial finite linear combination of eigenfunctions from a given eigenspace with fixed $\lambda_\gamma = -\frac{|\gamma|}{4} \equiv -\frac{l}{4}$, i.e.

$$f = \phi_l = \sum_{|\gamma| = l} C_\gamma \psi_\gamma \quad (\not\equiv 0). \tag{4.13}$$

Thus, we study branching from the eigenfunctions (4.13), where the weak expansion (4.10) is the key. Obviously, for $f \approx \phi_l(y)$, it can be violated in a small neighbourhood of the nodal (zero) set of $\phi_l(y)$ so that its structure and overall measure is of practical interest. Fortunately, according to (4.3), these eigenfunctions are simply derivatives (4.3) of the *analytic* radially symmetric rescaled kernel $F(|y|)$ of the fundamental solution (4.1). Therefore, at possible bifurcation points, the nodal set of such f in (4.13) is well understood, has *zero measure* and consists of a countable set of isolated sufficiently smooth hypersurfaces that can concentrate as $y \to \infty$, where

$$\phi_l(y) \to 0 \quad \text{as} \quad y \to \infty \text{ uniformly and exponentially fast.} \tag{4.14}$$

This allows us, returning to the key limit (4.10), to state the following result. For a

https://doi.org/10.1017/S0956792511000039 Published online by Cambridge University Press

function f given by (4.13), in the sense of distributions (see [10, Section 8.2]),

$$\frac{1}{n}\,(|f|^n - 1) \rightharpoonup \ln|f| \quad \text{as} \quad n \to 0^+. \tag{4.15}$$

According to (4.15), analysing the integral equation for f, we can use the fact that for any function $\phi \in L^1(\mathbb{R}^N)$ (and/or $\phi \in C_0(\mathbb{R}^N)$), as $n \to 0^+$,

$$\int_{\mathbb{R}^N} (|f(y)|^n - 1)\phi(y)\,\mathrm{d}y = n\left[\int_{\mathbb{R}^N} \ln|f(y)|\phi(y)\,\mathrm{d}y + o(1)\right]. \tag{4.16}$$

It follows from (4.11) that branching is possible under the following non-trivial kernel assumption: for $n = 0$,

$$\alpha - \frac{N}{4} = -\lambda_l = \frac{l}{4} \quad \Longrightarrow \quad \alpha_l(0) = \frac{N+l}{4}, \quad l \geqslant 0. \tag{4.17}$$

This gives the countable sequence of critical exponents $\{\alpha_l(n), \beta_l(n)\}$ (to be determined) of the similarity patterns (4.5) of the TFE for small $n > 0$.

By [9, Lemma 4.1], the kernel of the linearised operator

$$E_0 = \ker(\mathbf{B} - \lambda_l I) = \mathrm{Span}\,\{\psi_\beta,\ |\beta| = l\}$$

is finite-dimensional. Hence, denoting by E_1 the complementary (orthogonal to E_0) invariant sub-space, we set

$$f = \phi_l + V_1, \quad \text{where } \phi_l \in E_0 \text{ and } V_1 = \sum_{|\gamma|>l} c_\gamma \psi_\gamma \in E_1. \tag{4.18}$$

According to the known spectral properties of operator $\mathbf{B}$, we define P_0 and P_1, $P_0 + P_1 = I$, to be projections onto E_0 and E_1, respectively. We also introduce a perturbation of the parameter α by setting

$$\alpha_l(n) = \alpha_l(0) + \delta, \quad \text{with} \quad \delta = \delta(n). \tag{4.19}$$

This perturbation δ is obtained from the orthogonality condition by substituting into (4.11) and multiplying by ψ_γ^*. This gives

$$\delta(n) = c_l n + o(n), \tag{4.20}$$

where c_l is obtained from the system

$$\langle \mathscr{L}(\phi_l), \psi_\gamma^* \rangle = c_l, \quad |\gamma| = l. \tag{4.21}$$

Since, according to (4.18), ϕ_l is given by (4.13), (4.21) is an algebraic system for unknowns $\{C_\gamma\}$ and c_l. It can be solved, for instance, in radial geometries and in some other cases, including those where the dimension of the kernel is odd; even dimensions are known to need additional treatment (see more details in [17, App. A]). However, the total number of solutions of the non-variational system (4.21) remains unclear.

https://doi.org/10.1017/S0956792511000039 Published online by Cambridge University Press

Finally, setting

$$V_1 = nY + o(n), \tag{4.22}$$

we obtain, passing to the limit $n \to 0^+$, the following equation for Y:

$$\mathbf{B}Y = -c_l\phi_l + \mathscr{L}(\phi_l). \tag{4.23}$$

By Fredholm's theory, in view of the orthogonality, it admits a unique solution $Y \in E_1$.

In general, the above analysis shows that up to solvability of the non-linear algebraic systems the TFE admits a countable set of different source-type similarity solutions (4.5) at least for small $n > 0$, where the parameters $\alpha_l(n)$ are given by

$$\alpha_l(n) = \frac{N+l}{4} + c_l n + o(n) \quad \text{as} \quad n \to 0^+; \quad l = 0, 1, 2, \dots. \tag{4.24}$$

At $n = 0$, these solutions originate from suitable eigenfunctions of the linear operator in (4.1). The global extensions of these n-branches of similarity solutions for larger $n > 0$ represent a difficult open problem and are treated numerically later on.

4.3 Non-linear eigenfunctions of TFE in one dimension

We consider the CP for the 1D TFE with continuous, compactly supported initial data,

$$u_t = -(|u|^n u_{xxx})_x \quad \text{in} \quad \mathbb{R} \times \mathbb{R}_+, \quad u(x,0) = u_0(x) \in C_0(\mathbb{R}). \tag{4.25}$$

Then, for $N = 1$, the *non-linear eigenvalue problem* for the elliptic equation (4.6) is formulated as follows:

$$\boxed{-(|f|^n f''')' + \frac{1-\alpha n}{4} y f' + \alpha f = 0 \quad \text{in} \quad \mathbb{R}, \quad f(y) \not\equiv 0, \quad f \in C_0(\mathbb{R}).} \tag{4.26}$$

The problem (4.26) is naturally connected with self-similarity of *second kind*. Here, the admitted values of the parameters $\{\alpha_l(n), l \geqslant 0\}$ (non-linear eigenvalues) are obtained not by pure dimensional analysis, but via solvability of this non-linear ODE in a given functional class $C_0(\mathbb{R})$ of compactly supported functions satisfying the condition of maximal regularity. The term *similarity of the second type* was introduced by Zel'dovich in 1956 [29].

Note that for $n = 0$, we pose (4.26) in $L^2_\rho(\mathbb{R})$, where we replace the last condition by

$$f \in L^2_\rho(\mathbb{R}).$$

This is then a standard *linear eigenvalue problem* for a non-self-adjoint operator with the point spectrum (4.2) and a complete-closed set of eigenfunctions $\{\psi_\beta\}$ given in (4.3), [8].

The first non-linear eigenvalue–eigenfunction pair $\{F_0, \alpha_0\}$ of (4.26) has been proved to exist for $n \in (0, 1]$ (see [10, Section 9]). In this case, the first eigenvalue is

$$\alpha_0(n) = \frac{N}{4+nN}\bigg|_{N=1} = \frac{1}{4+n}. \tag{4.27}$$

https://doi.org/10.1017/S0956792511000039 Published online by Cambridge University Press

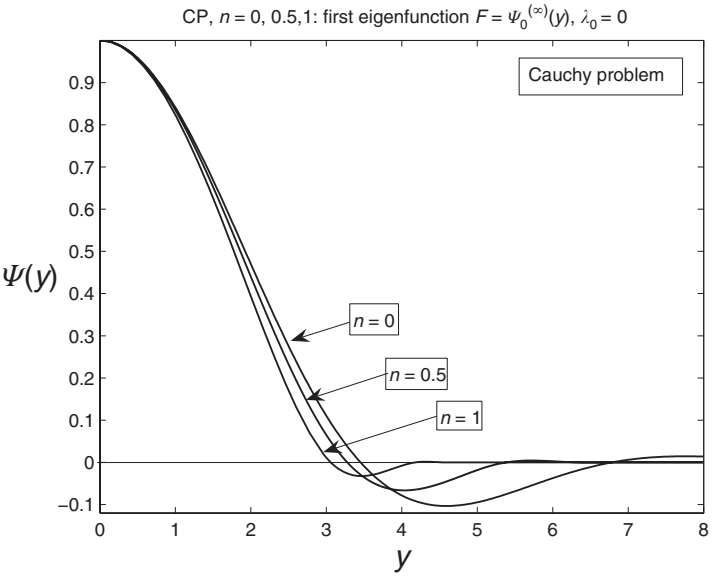

(a) Eigenfunctions

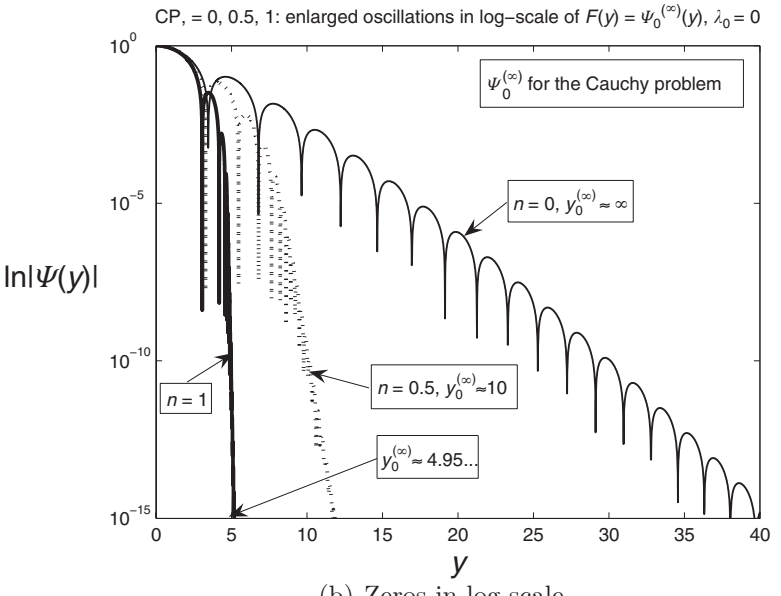

(b) Zeros in log-scale

FIGURE 5. The first eigenfunction of (4.26) and (4.27) for $n = 0$, 0.5 and 1.

In view of the highly oscillatory nature of the profiles near interfaces, even identifying numerically the position of interfaces is not an easy problem. Therefore, we begin with Figure 5, where the first even non-linear eigenfunction is presented for $n = 0$, $\frac{1}{2}$ and 1. A careful study of their zero structure in the log-scale in Figure 5(b) allows us to find an approximate and rather rough interface location, according to expansion (3.5), which

https://doi.org/10.1017/S0956792511000039 Published online by Cambridge University Press

yields

$$\ln|f(y)| = \frac{3}{n}\,\ln(y_0 - y) + \ln|\varphi(\ln(y_0 - y)| + \cdots \tag{4.28}$$

For $n = 0$, the expansion is exponential (cf. (5.12) in Part II) and entirely different, which is seen in Figure 5(b); recall that the regularisation, such as (3.12), eventually enters the expansion for $|f|$ very small.

In what follows, we use the parameterisation:

$$F_l(0) = 1, \;\; l = 0, 2, 4, \ldots; \quad F_l'(0) = 1, \;\; l = 1, 3, \ldots \tag{4.29}$$

We then obtain, respectively,

$$\alpha_1 = 0.2534\ldots, \quad \alpha_2 = 0.320\ldots \quad (n = 1). \tag{4.30}$$

In addition, numerics show that $\alpha_3 \approx 0.38$ for $n = 1$.

The results of an accurate numerical study of the first four non-linear eigenfunctions for $N = 1$ and various $n \in [0, 2]$ are presented in Figure 6. Further, eigenfunctions are very difficult to obtain numerically, to say nothing about an analytical proof of their existence.

The first n-branch, according to (4.27), has the explicit form

$$\alpha_0(n) = \tfrac{1}{4+n}, \quad n \in [0, 3).$$

Other n-branches cannot be obtained explicitly. According to the n-branching approach, all these branches originate at the eigenvalues of the linear problem (4.2), i.e.

$$\alpha_l(0) = -\lambda_{l+1} = \frac{l+1}{4} \quad \text{for} \quad l = 0, 1, 2, \ldots, \tag{4.31}$$

and moreover, after scaling, we may assume that at $n = 0$ the similarity profiles $F_l(y)$ coincide with the eigenfunctions (4.3), and hence by continuity mimic their geometric shapes for $n > 0$.

Figure 7 shows the actual numerical construction of the first four n-branches, and even these involve technical difficulties. Note that at the critical heteroclinic bifurcation value (3.7), the similarity profiles $F_l(y)$ are supposed to lose their oscillatory behaviour at the interface and become 'finite oscillatory' (a finite number of isolated zeros near interfaces) for $n > n_{\rm h}$ (or even non-oscillatory at all) (see [10, Section 7.2]).

The analytical difficulties for the eigenvalue problem (4.26) already begin with $l = 1$, i.e. with the dipole profile $F_1(y)$. This study has a well-developed history (see [3, 6, 7] and references therein), but still there are no definite results of existence and uniqueness of F_1 in the CP (nor the FBP) setting.

We end this section with the following:

Conjecture 4.1 (i) *For any $n \in (0, n_{\rm h})$, the non-linear eigenvalue problem* (4.26) *admits a countable set of sufficiently smooth solutions of maximal regularity*[2]

$$\Phi = \{F_l(y), \; l = 0, 1, 2, \ldots\}, \tag{4.32}$$

[2] More details on this are given in [10].

https://doi.org/10.1017/S0956792511000039 Published online by Cambridge University Press

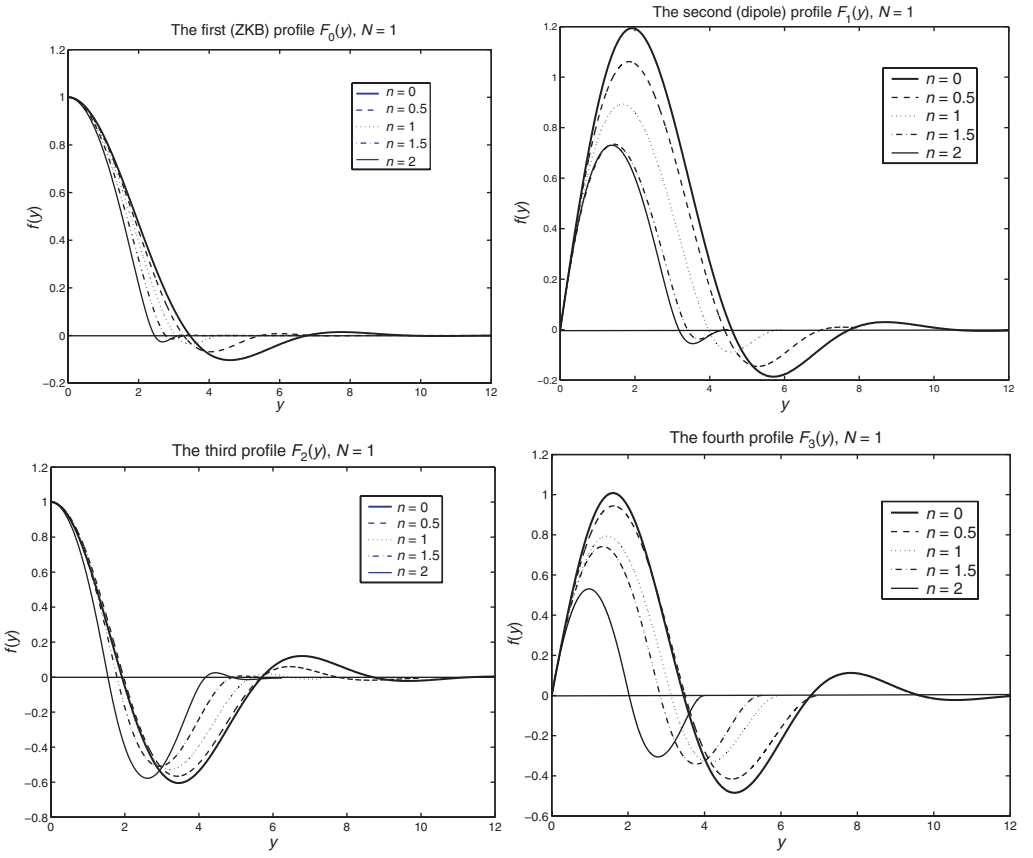

FIGURE 6. Illustrative numerical solutions for the first four non-linear eigenfunctions $F_l(y)$, $l = 0, 1, 2, 3$, shown for selected n in 1D $N = 1$. The corresponding behaviour of the eigenvalues is shown in Figure 7. The regularisation (3.12) with $\delta = 10^{-2}$ was used in the numerical shooting scheme, where the even numbered profiles satisfy $F_l(0) = 1, F_l'(0) = F_l'''(0) = 0$, whilst the odd numbered profiles have $F_l'(0) = 1, F_l(0) = F_l''(0) = 0$.

where the non-linear eigenvalues $\{\alpha_l\}$ *form a strictly increasing sequence and*

$$\alpha_l \to \tfrac{1}{n} \quad as \quad l \to \infty. \tag{4.33}$$

(ii) *The eigenfunction subset* (4.32) *is evolutionarily complete in* $C_0(\mathbb{R})$ *for the TFE* (4.25), *i.e. for any* $u_0 \neq 0$, *there exists a finite* $l \geqslant 0$ *and a constant* $b = b(u_0) \neq 0$ *such that*

$$u(x,t) = t^{-\alpha_l}\left[bF_l(x/t^{\beta_l}|b|^{n/4}) + o(1)\right] \quad as \quad t \to \infty. \tag{4.34}$$

We expect that an analogous countable set of radially symmetric similarity solutions exists for the TFE (1.8) in any dimension $N \geqslant 2$, though numerical calculations become much more difficult than for $N = 1$. Moreover, the branching approach in Section 4.2 shows that there are many other non-radial similarity solutions that have a more complicated geometry, but which for small $n > 0$ mimic the eigenfunctions (4.3).

https://doi.org/10.1017/S0956792511000039 Published online by Cambridge University Press

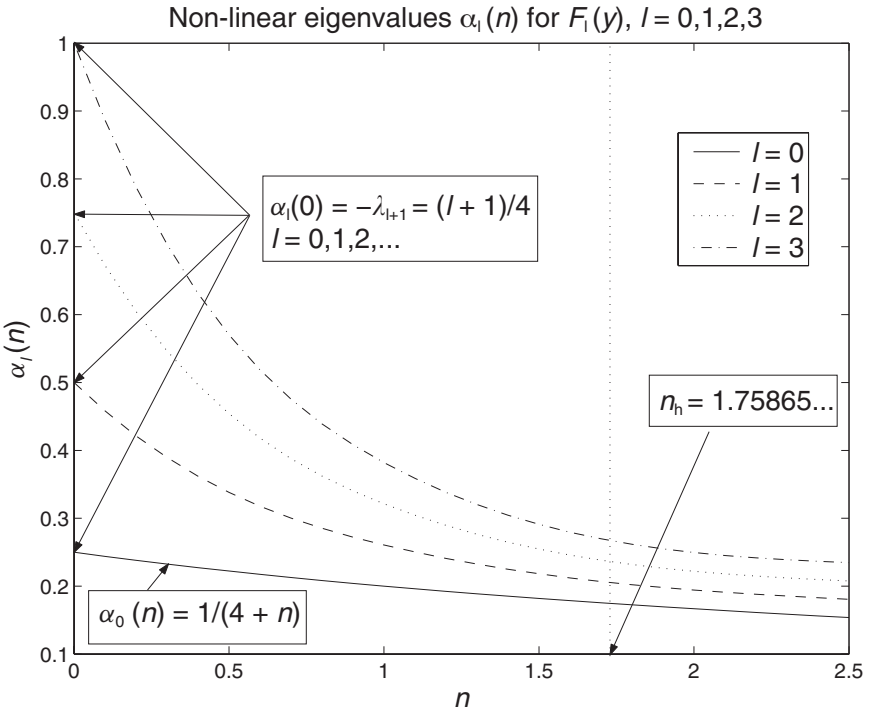

FIGURE 7. The actual n-branches of the first four non-linear eigenvalues $\alpha_l(n)$, $l = 0, 1, 2, 3$, constructed numerically.

The evolution completeness of non-linear eigenfunctions is known rigorously for the PME

$$u_t = (|u|^n u)_{xx} \quad (n > 0) \tag{4.35}$$

in a bounded interval [14]; also see [17] for results in $\mathbb{R}^N$ for initial data $u_0 \in C_0(\mathbb{R}^N)$ and on an n-branching technique. The existence of a countable set of radial similarity solutions of the PME (4.35) in $\mathbb{R}^N \times \mathbb{R}_+$ was proved by Hulshof [23].

5 On non-linear p-bifurcations

5.1 Semi-linear Cahn–Hilliard (CH) equation: Countable set of critical exponents

In order to explain the essence of the non-linear bifurcation analysis, we first digress to the stable CH equation (1.6), for which the analysis is much simpler (cf. [12, 21]).

Namely, studying the behaviour as $t \to +\infty$, we perform the standard scaling

$$u(x,t) = (1+t)^{-\frac{1}{2(p-1)}} v(y,\tau), \quad y = x/(1+t)^{\frac{1}{4}}, \quad \tau = \ln(1+t), \tag{5.1}$$

where $v(y,\tau)$ solves the following rescaled equation:

$$v_\tau = -\Delta^2 v + \tfrac{1}{4}\, y \cdot \nabla v + \tfrac{1}{2(p-1)}\, v + \Delta(|v|^{p-1}v) \equiv \mathbf{B}v + c_0 v + \Delta(|v|^{p-1}v). \tag{5.2}$$

It then follows from (4.2) that a centre manifold behaviour is formally possible in critical

https://doi.org/10.1017/S0956792511000039 Published online by Cambridge University Press

cases (2.10) only:

$$c_0 = \frac{1}{2(p-1)} - \frac{N}{4} = \frac{l}{4} \quad \Longrightarrow \quad p = p_l = 1 + \frac{2}{N+l} \quad (l \geqslant 0). \tag{5.3}$$

Checking the necessary condition of such a centre manifold behaviour and looking, say, for a solution restricted to the centre eigenspace,

$$v(y,\tau) = a_\gamma(\tau)\psi_\gamma(y) + w, \quad w \perp \psi_\gamma, \quad \sup_y |w(y,\tau)| = o(a_\gamma(\tau)) \text{ as } \tau \to \infty, \tag{5.4}$$

and substituting into (5.2) yields on multiplication by ψ_γ^* (see [8] for details),

$$\dot{a}_\gamma(\tau) = \mu_\gamma |a_\gamma|^{p-1} a_\gamma + \cdots, \quad \text{where} \quad \mu_\gamma = \langle \Delta|\psi_\gamma|^{p-1}\psi_\gamma, \psi_\gamma^* \rangle \equiv \langle |\psi_\gamma|^{p-1}\psi_\gamma, \Delta\psi_\gamma^* \rangle. \tag{5.5}$$

Since $\psi_\gamma^*(y)$ is a γ-degree polynomial [8], we then conclude that the necessary condition of existence of such a centre sub-space behaviour is as follows:

$$\mu_\gamma \neq 0 \quad \text{at least, for } |\gamma| \geqslant 2. \tag{5.6}$$

Note that in the limit $p \to 1$ the following holds:

$$\mu_\gamma = 1 \quad \text{by bi-orthonormality of eigenfunctions} \tag{5.7}$$

so that (5.6) is true for $l \gg 1$ through continuity of the integral relative to the parameter p.

Eventually, the centre sub-space behaviour (5.5) generates the following asymptotic patterns for the CH equation (1.6):

$$u_\gamma(x,t) \sim C_\gamma (t \ln^2 t)^{-\frac{N+l}{4}} \psi_\gamma \left(\frac{y}{t^{1/4}} \right) + \cdots \quad \text{as} \quad t \to \infty \quad (l = |\gamma| \geqslant 2), \tag{5.8}$$

where constants C_γ are independent of initial data u_0. Of course, according to (4.3), all such centre sub-space patterns (5.8) have zero mass, which is a necessary condition to create an extra logarithmically decaying factor therein.

5.2 Local bifurcations from p_l

We now return to the VSS of TFE with the stable PME term (1.1) and perform a formal *non-linear* version of a p-bifurcation (branching) analysis for $n > 0$. As usual, according to the classic branching theory [25, 27], a justification (if any) is performed for the equivalent quasi-linear integral equation with compact operators. For simplicity, we present computations for the differential setting.

Thus, we consider the elliptic PDE (2.2). The critical exponents $\{p_l\}$ are then determined from the equality (q.v. (5.3))

$$\alpha \equiv \frac{1}{2p_l(n) - (n+2)} = \alpha_l(n) \quad \Longrightarrow \quad p_l(n) = \frac{n+2}{2} + \frac{1}{2\alpha_l(n)} \quad (l \geqslant 0). \tag{5.9}$$

In particular, for the semi-linear case $n = 0$, we have $\alpha_l(0) = \frac{N+l}{4}$ from (4.17) so that (5.9) leads to (5.3), i.e. to the known sequence of critical exponents (2.10).

https://doi.org/10.1017/S0956792511000039 Published online by Cambridge University Press

We next use an expansion relative to the small parameter $\varepsilon = p_0 - p$, i.e. as $\varepsilon \to 0$,

$$\alpha = \frac{1}{2p_l - (n+2) - 2\varepsilon} = \alpha_l + 2\alpha_l^2\varepsilon + \cdots,$$

$$\beta = \frac{1 - n\alpha_l}{4} + c_l\varepsilon + \cdots, \quad c_l = \frac{1 - n\alpha_l}{4}\Big[n + 2 + \frac{1}{\alpha_l} - \frac{2}{1 - n\alpha_l}\Big].$$

Substituting these expansions and the last one in (4.9) into (2.2) and performing the same standard linearisation yields

$$\mathbf{A}_n(f) + \Delta(|f|^{p_l} f) + \varepsilon[-\Delta(|f|^{p_l} f \ln |f|) + \mathscr{L}_1 F] + O(\varepsilon^2) = 0, \tag{5.10}$$

where

$$\mathscr{L}_1 = c_l y \cdot \nabla + 2\alpha_l^2 I$$

is a linear operator and $\mathbf{A}_n$ is the non-linear rescaled operator (4.6) of the pure TFE with the parameter $\alpha = \alpha_l(n)$ (an eigenvalue), for which there exists the corresponding similarity profile $F_l(y)$ (the non-linear eigenfunction).

We now make use of the invariant scaling of the operator $\mathbf{A}_n$ by setting

$$f(y) = bF(y/b^{\frac{n}{4}}) \quad (b > 0), \tag{5.11}$$

where $b = b(\varepsilon) > 0$ is a small parameter satisfying

$$b(\varepsilon) \to 0 \quad \text{as} \quad \varepsilon \to 0, \tag{5.12}$$

which is to be determined. Substituting (5.11) into (5.10) and omitting all higher order terms (including the one with the logarithmic multiplier $\ln |b(\varepsilon)|$) yields

$$\mathbf{A}_n(F) + b^{p_l - \frac{n}{2}}\Delta(|F|^{p_l} F) + \varepsilon\mathscr{L}_1 F = 0. \tag{5.13}$$

Finally, we perform linearisation about the non-linear eigenfunction $F_l(y)$ by setting

$$F = F_l + Y.$$

This yields the following linear non-homogeneous problem:

$$\mathbf{A}_n'(F_l)Y + b^{p_l - \frac{n}{2}}\Delta(|F_l|^{p_l} F_l) + \varepsilon\mathscr{L}_1 F_l = 0, \tag{5.14}$$

where the derivative is given by

$$\mathbf{A}_n'(F)Y = -\nabla \cdot \left[|F|^n \left(\frac{n}{F}(\nabla\Delta F)Y + \nabla\Delta Y\right)\right] + \beta_l y \cdot \nabla Y + \alpha_l Y.$$

The remaining analysis depends on assumed 'sufficiently good' spectral properties of the linearised operator $\mathbf{A}_n'(F_l)$. It is noted that this is a difficult singular elliptic operator with non-constant coefficients. Moreover, linearisation is performed about the *a priori* unknown non-linear eigenfunction F_l. Therefore, we have to assume the best spectral properties in order just to proceed with the more difficult idea of non-linear bifurcations.

https://doi.org/10.1017/S0956792511000039 Published online by Cambridge University Press

Here, we mainly follow the lines of a similar analysis performed for the FBP case in [19, Section 2], where the operator $\mathbf{A}'_n(F_l)$ for $n = 1$ turns out to possess a (Friedrichs') self-adjoint extension with compact resolvent and discrete spectrum. However, it was proved in [19, Appendix A] that such a self-adjoint extension does not exist for the oscillatory $F(y)$. As such, we use the more general theory of non-self-adjoint operators, with Riesz bi-orthogonal bases etc. (see, e.g. [22]). A proper functional setting of this operator is more straightforward for $N = 1$ (and in the radial setting), where, using the behaviour of $F(y) \to 0$ as $y \to 1$, it is possible to check whether the resolvent is compact in a suitable weighted L^2 space. In general, this is a difficult problem (see below).

In order to proceed, we assume that a proper functional setting is available for $\mathbf{A}_n$, and so we deal with operators having solutions with 'minimal' singularities at the boundary of the support S_l, where the operator is degenerate and singular. Namely, we assume that $\mathbf{A}'_n(F_l)$ has a discrete spectrum with a complete, closed set of eigenfunctions denoted again by $\{\psi_\gamma\}$ and finite-dimensional kernel. We also assume that we are able to determine the spectrum, eigenfunctions $\{\psi^*_\gamma\}$ and the kernel of the adjoint operator $(\mathbf{A}'_n(F_l))^*$, which is defined in a natural way using the topology of the dual space L^2 and having the same point spectrum (the latter is true for compact operators in a suitable space [24, Ch. 4]).

Further, we assume that there exists the orthogonal sub-space $\mathrm{Span}\{\psi_\gamma, |\gamma| > l\}$ of eigenfunctions of $\mathbf{A}'_n(F_l)$. We look for solutions of (5.14) in the form

$$Y = \phi_l + w,$$

where ϕ_l belongs to the kernel and hence is analogously given by (4.13), whilst w belongs to the orthogonal complement of the kernel. In doing so, we need to transform (5.14) into an equivalent integral equation with compact operators, but for convenience, we continue our computations using the differential version (see additional details in [21, Section 3]).

Thus, multiplying (5.14) by ψ^*_γ with any $|\gamma| = l$ in L^2 and, if necessary, integrating by parts the differential term $y \cdot \nabla F_l$ in $\mathscr{L}_1 F_l$, we obtain the following orthogonality condition of solvability (Lyapunov–Schmidt's branching equation [27, Section 27]):

$$b^{p_l - \frac{n}{2}} \langle \Delta(|F_l|^{p_l - 1} F_l), \psi^*_\gamma \rangle = -\varepsilon \langle \mathscr{L}_2 F_l, \psi^*_\gamma \rangle \quad \text{for all} \quad |\gamma| = l. \tag{5.15}$$

These are algebraic equations for the expansion coefficients $\{C_\gamma\}$ in (4.13) and the parameter $b = b(\varepsilon)$. Similar to (5.5), one needs to check whether the constants are non-zero,

$$\langle \Delta(|F_l|^{p_l - 1} F_l), \psi^*_\gamma \rangle \neq 0 \quad \text{and} \quad \langle \mathscr{L}_2 F_l, \psi^*_\gamma \rangle \neq 0, \tag{5.16}$$

which is not a simple problem and can lead to restrictions for such a behaviour. The analysis is much simpler if the kernel is one dimensional, which always happens in the radial geometry where we deal with ordinary differential operators. Then (5.15) is a single and easily solved algebraic equation, for which the 'transversality' problem (5.16) also occurs.

Under the conditions (5.16), the parameter $b(\varepsilon)$ in (5.11) for $p \approx p_0$ is given by

$$b(\varepsilon) \sim [\gamma_l (p_l - p)]^{\frac{2\alpha_l}{1 + 2\alpha_l}}. \tag{5.17}$$

https://doi.org/10.1017/S0956792511000039 Published online by Cambridge University Press

The direction of each p_l-branch and whether the bifurcation is sub- or super-critical depends on the sign on the coefficient γ_l that follows from (5.15). This can be checked numerically only, but, in general, we expect that most of these non-linear bifurcations are *sub-critical*,[3] so the p_l-branches exist for $p < p_l$ (at least, locally; see [16] for nonmonotone 'closed-loop' p-branches for TFE with absorption).

For $n = 0$, a rigorous justification of this bifurcation analysis can be found in [21, Section 6], where a countable number of p-branches was shown to originate at bifurcation points (2.10) and was detected on the basis of known spectral properties of the corresponding linear operator in (4.1) (see details in [8]). For $n > 0$, as we have seen, the justification needs spectral properties of the linearised operator $\mathbf{A}'_n(F_l)$, as well as the corresponding adjoint $(\mathbf{A}'_n(F_l))^*$, which is difficult for non-radial, non-linear eigenfunctions F_l and is an open problem. In particular, it would be important to know that the bi-orthonormal eigenfunction subset $\{\psi_\gamma\}$ of the operator $\mathbf{A}'_n(F_l)$ is complete and closed in a weighted L^2-space or in some specially defined closed sub-space (for $n = 0$, such results are available [8]). We expect that for $n \approx 0$, there exist critical exponents for TFE with absorption that are close to those in (2.10) at $n = 0$. This can be checked by standard branching-type calculus (see [17, Appendix A]), where non-linear eigenfunctions of the rescaled PME in $\mathbb{R}^N$ were studied by a branching approach.

6 Towards global extensions of p-branches

6.1 Examples of various profiles

Recall that, for $p \neq p_0$ in the ODE (3.1), we still have a 2D bundle at the singular interface point (3.9), but now, for even profiles, we also need to satisfy two symmetry boundary conditions at the origin:

$$f'(0) = f'''(0) = 0. \tag{6.1}$$

Therefore, unlike the third-order problem (3.10) and (3.11) in the critical case $p = p_0$, we cannot expect continuous sets of solutions. Actually, as was shown in [10–12, 21], in these non-critical cases, there occurs a countable set of p-branches of similarity profiles that originate at the standard (for $n = 0$) or non-linear bifurcation points $\{p_l\}$ as explained in Section 5. The global behaviour of such p-branches can be complicated and we do not intend to study such delicate open questions on their properties in any detail, restricting ourselves to examples only.

In Figure 8, we present some VSS profiles $f(y)$ for $N = 1$ in two cases: $n = 1$ and $p = 3 < p_0 = 4$ in Figure 8(a) and $n = \frac{1}{2}$, $p = 2$ in Figure 8(b). In Figure 8(b), we also show the first dipole profile $f_1(y)$ that, instead of (6.1), satisfies the anti-symmetry conditions at the origin,

$$f(0) = f''(0) = 0 \quad \Longrightarrow \quad f(-y) \equiv -f(y). \tag{6.2}$$

Note an important feature of such compactly supported profiles that is seen in the

[3] Cf. [21], where a bi-harmonic equation with *absorption* was studied, as well as [16] for the TFE with absorption; the present diffusion operator is also negative in a natural sense. For positive (source-type) operators, bifurcations are *super-critical* [12, 18].

https://doi.org/10.1017/S0956792511000039 Published online by Cambridge University Press

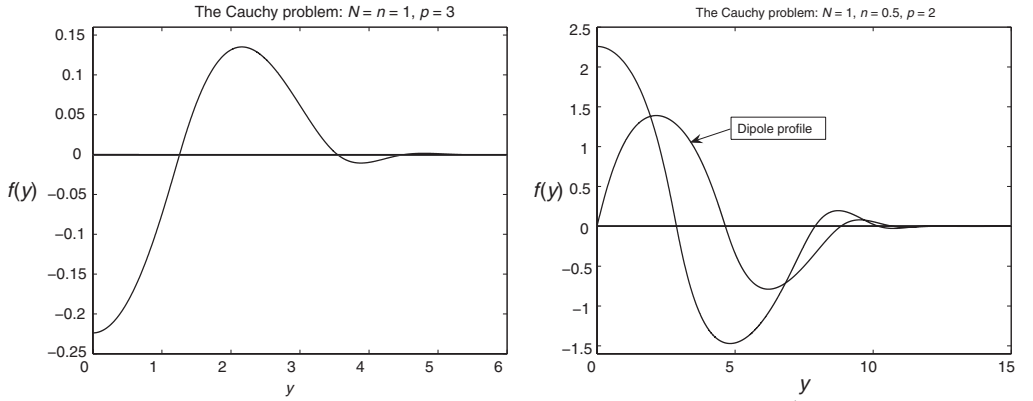

(a) $n = 1$, $p = 3$ (b) $n = \frac{1}{2}$, $p = 2$

FIGURE 8. Examples of VSS profile for the CP satisfying (3.1) and (6.1) for $N = 1$; (a) $n = 1$, $p = 3$, and (b) $n = \frac{1}{2}$, $p = 2$.

figures: by (2.7), *their mass must be zero*. This necessary condition affects the VSS similarity profiles so that it gets difficult to distinguish in Figure 8 their Sturmian-like properties on the numbers of dominant extrema and transversal zeros (if these apply at all). Note that the orthogonality property in (2.7) is perfectly valid for the eigenfunctions (4.3) for $n = 0$ (see (4.8)), which made it possible to develop the above branching theory.

6.2 p-bifurcation branches: numerics

The semi-linear case, $n = 0$, although simpler, correctly describes the expected general behaviour of the p-branches, at least for sufficiently small $n > 0$ (bearing in mind that a continuous 'homotopic' deformation as $n \to 0$ is observed in a number of papers mentioned above). Thus, Figure 9 illustrates this sub-critical case for even symmetry conditions (6.1) at the origin. The branches are seen to remain distinct, which contrasts markedly with the supercritical case [10, 12], where the branches are increasing with p, so that the p_2 and higher branches 'intersect' the vertical p_0 branch, $\{p = 3\}$ at points (profiles) f with the zero mass as in (2.7).

In Figure 9(a), we observe a strong, almost vertical, growth of these p-branches that bifurcate, respectively, at

$$p_2 = 1 + \tfrac{2}{1+2} = \tfrac{5}{3}, \quad p_4 = 1 + \tfrac{2}{1+4} = \tfrac{7}{5}, \quad p_6 = 1 + \tfrac{2}{1+6} = \tfrac{9}{7}. \tag{6.3}$$

This is not surprising, since the ODE (3.1) for $N = 1$ and $n = 0$ assumes, as $p \to 1^-$, balancing the terms

$$\cdots + (|f|^{p-1}f)'' + \cdots + \frac{1}{2(p-1)}\, f = 0 \implies f = C\,\hat{f}, \ \text{where } C(p) \sim (p-1)^{-\frac{1}{p-1}} \tag{6.4}$$

(the scaled function $\hat{f}(y)$ is then supposed to be uniformly bounded, probably up to slower growing factors). Therefore, by (6.4) $f(y)$ has super-exponential growth as $p \to 1^+$. Since the bifurcation values in (6.3) are already sufficiently close to 1 and the bifurcations

https://doi.org/10.1017/S0956792511000039 Published online by Cambridge University Press

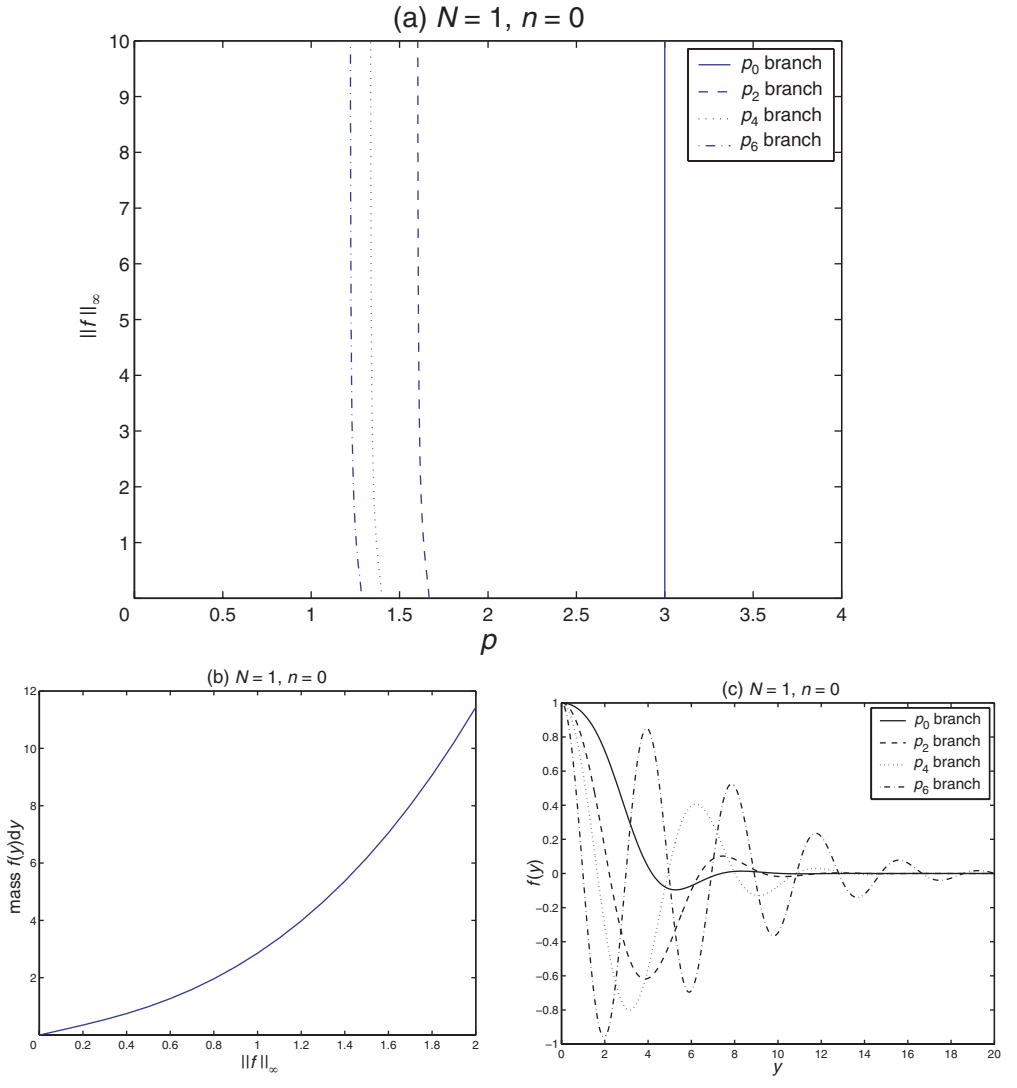

FIGURE 9. (Colour online) The bifurcation p-diagram and associated plots for the CP case, when $N = 1, n = 0$: (a) shows the p-bifurcation branches emanating from the critical exponents $p = p_l = 1 + \frac{2}{1+l}$ on the p-axis. The first four (even) branches $l = 0, 2, 4, 6$ are plotted; (b) illustrates the monotonicity of the mass of solutions in the critical case $p = p_0 = 3$; whilst (c) shows selected profiles on the four branches in (a) that have $||f||_\infty = 1$.

are sub-critical, these explain such a strong growth of all the p-bifurcation branches in Figure 9(a).

In the non-linear case $n > 0$, such a convincing justification of the general p-diagram is not available. Indeed, as we have shown in the previous section, in the simplest case $l = 0$, i.e. $p = p_0$, the bifurcation of this vertical (in p) branch occurs from a non-linear eigenfunction, which is the scaled source-type profile of the non-linear thin film operator. Other non-linear eigenfunctions of the thin film operator are still unknown, possibly

https://doi.org/10.1017/S0956792511000039 Published online by Cambridge University Press

excluding the second dipole-like eigenfunction. We expect that the discrete nature of the p-bifurcation branches discovered in [12] for $n = 0$ remains valid for small $n > 0$, where the non-linear branching points cannot be calculated explicitly as in (2.10) and follows from a complicated non-linear eigenvalue problem for the thin film operator.

7 Discussion

In this paper we have presented the main ideas with regard to describing a class of similarity solutions for the CP of the fourth-order TFE with a stable parabolic term (1.1). We define the CP as that of admitting solutions of maximal regularity.

The local asymptotic properties near an interface were described in Section 3 for the quasi-linear range $n \in (0, n_{\rm h})$, where $n_{\rm h}$ is the point of a *heteroclinic bifurcation* for a related non-linear ODE. In this range of n, the rescaled ODE exhibits a unique stable periodic motion describing generic changing sign properties of more general solutions. As we shall see in Part II, these asymptotics contrast markedly with the more standard and reasonably well-known behaviours (since the 1990s) for FBPs.

Also, in Section 3 we studied for the CP the critical case

$$p = p_0 = n + 1 + \frac{2}{N},$$

where we detected continuous branches of similarity profiles. In Section 4, the n-branching theory was developed for the similarity solutions of the 1D pure TFE

$$u_t = -(|u|^n u_{xxx})_x.$$

Specifically, the branching of non-linear similarity profiles from eigenfunctions of the linear rescaled operator at $n = 0$. This allowed us in Section 5 to reveal a countable sequence of critical exponents $\{p_l\}$ of the original stable TFE (1.1) and to describe similarity solutions for $p \neq p_0$.

As some of the conclusions remain formal, we have posed several open problems for future research.

In Part II we turn our attention to the FBP setting, where the CP will emerge as a suitable limit of FBP problems. We mention that this *limit property* affords an alternative definition of solutions of the CP, which complements the existing ones of *maximal regularity* at interfaces or via a smooth analytic 'homotopy' deformation to the bi-harmonic equation (1.9).

Acknowledgement

The authors would like to thank both anonymous Referees for careful reading our manuscript and several useful suggestions.

References

[1] Bernis, F. (1988) Source-type solutions of fourth order degenerate parabolic equations. In: W.-M. Ni, L. A. Peletier & J. Serrin (editors), *Proc. Microprogram Nonlinear Diffusion Eqs Equilibrium States*, Vol. 1, MSRI Publications, New York, NY, USA, pp. 123–146.

[2] Bernis, F. & Friedman, A. (1990) Higher order nonlinear degenerate parabolic equations. *J. Differ. Equ.* **83**, 179–206.

[3] Bernis, F., Hulshof, J. & King, J. R. (2000) Dipoles and similarity solutions of the thin film equation in the half-line. *Nonlinearity* **13**, 413–439.

[4] Bernis, F. & McLeod, J. B. (1991) Similarity solutions of a higher order nonlinear diffusion equation. *Nonlinear Anal.* **17**, 1039–1068.

[5] Bernis, F., Peletier, L. A. & Williams, S. M. (1992) Source-type solutions of a fourth order nonlinear degenerate parabolic equation. *Nonlinear Anal. Theory Methods Appl.* **18**, 217–234.

[6] Bowen, M., Hulshof, J. & King, J. R. (2001) Anomalous exponents and dipole solutions for the thin film equation. *SIAM J. Appl. Math.* **62**, 149–179.

[7] Bowen, M. & Witelski, T. P. (2006) The linear limit of the dipole problem for the thin film equation. *SIAM J. Appl. Math.* **66**, 1727–1748.

[8] Egorov, Yu. V., Galaktionov, V. A., Kondratiev, V. A. & Pohozaev, S. I. (2004) Asymptotic behaviour of global solutions to higher-order semilinear parabolic equations in the supercritical range. *Adv. Difference Equ.* **9**, 1009–1038.

[9] Evans, J. D., Galaktionov, V. A. & King, J. R. (2007a) Blow-up similarity solutions of the fourth-order unstable thin film equation. *Eur. J. Appl. Math.* **18**, 195–231.

[10] Evans, J. D., Galaktionov, V. A. & King, J. R. (2007b) Source-type solutions for the fourth-order unstable thin film equation. *Eur. J. Appl. Math.* **18**, 273–321.

[11] Evans, J. D., Galaktionov, V. A. & King, J. R. (2007c) Unstable sixth-order thin film equation. I. Blow-up similarity solutions; II. Global similarity patterns. *Nonlinearity* **20**, 1799–1841, 1843–1881.

[12] Evans, J. D., Galaktionov, V. A. & Williams, J. F. (2006) Blow-up and global asymptotics of the limit unstable Cahn–Hilliard equation. *SIAM J. Math. Anal.* **38**, 64–102.

[13] Ferreira, R. & Bernis, F. (1997) Source-type solutions to thin-film equations in higher dimensions. *Eur. J. Appl. Math.* **8**, 507–534.

[14] Galaktionov, V. A. (2004) Evolution completeness of separable solutions of non-linear diffusion equations in bounded domains. *Math. Methods Appl. Sci.* **27**, 1755–1770.

[15] Galaktionov, V. A. (2007) Sturmian nodal set analysis for higher-order parabolic equations and applications. *Adv. Difference Equ.* **12**, 669–720.

[16] Galaktionov, V. A. (2010) Very singular solutions for thin film equations with absorption. *Studies Appl. Math.* **124**, 39–63 (arXiv:0109.3982).

[17] Galaktionov, V. A. & Harwin, P. J. (2005a) On evolution completeness of nonlinear eigenfunctions for the porous medium equation in the whole space. *Adv. Difference Equ.* **10**, 635–674.

[18] Galaktinov, V. A. & Harwin, P. J. (2005b) Non-uniqueness and global similarity solutions for a higher-order semilinear parabolic equation. *Nonlinearity* **18**, 717–746.

[19] Galaktionov, V. A. & Harwin, P. J. (2009) On centre subspace behaviour in thin film equations. *SIAM J. Appl. Math.* **69**, 1334–1358 (an earlier preprint in arXiv:0901.3995v1).

[20] Galaktionov, V. A. & Svirshchevskii, S. R. (2007) *Exact Solutions and Invariant Subspaces of Nonlinear Partial Differential Equations in Mechanics and Physics*, Chapman & Hall/CRC, Boca Raton, FL, USA.

[21] Galaktionov, V. A. & Williams, J. F. (2004) On very singular similarity solutions of a higher-order semilinear parabolic equation. *Nonlinearity* **17**, 1075–1099.

[22] Gohberg, I., Goldberg, S. & Kaashoek, M. A. (1990) *Classes of Linear Operators*, Vol. 1; *Operator Theory: Advances and Applications*, Vol. 49, Birkhäuser Verlag, Basel, Switzerland/Berlin, Germany.

[23] Hulshof, J. (1991) Similarity solutions of the porous medium equation with sign changes. *J. Math. Anal. Appl.* **157**, 75–111.

[24] Kolmogorov, A. N. & Fomin, S. V. (1976) *Elements of the Theory of Functions and Functional Analysis*, Nauka, Moscow, Russia.
[25] Krasnosel'skii, M. A. & Zabreiko, P. P. (1984) *Geometrical Methods of Nonlinear Analysis*, Springer-Verlag, Berlin, Germany.
[26] Perko, L. (1991) *Differential Equations and Dynamical Systems*, Springer-Verlag, New York, USA.
[27] Vainberg, M. A. & Trenogin, V. A. (1974) *Theory of Branching of Solutions of Non-Linear Equations*, Noordhoff International Publishing, Leiden, Netherlands.
[28] Wu, Z., Zhao, J., Yin, J. & Li, H. (2001) *Nonlinear Diffusion Equations*, World Scientific Publishing Company, River Edge, NJ, USA.
[29] Zel'dovich, Ya. B. (1956) The motion of a gas under the action of a short-term pressure shock. *Akust. Zh.*, **2**, 28–38; *Sov. Phys. Acoust.* **2**, 25–35.